

Fragmentation analysis of compound nuclei formed in ^{16}O and ^{48}Ca induced reactions

Amandeep Kaur^{1,*}, Jagdeep Kaur², Rita Chhetri², and Manoj K. Sharma³

¹Chitkara University Institute of Engineering and Technology, Chitkara University, Punjab, India

²Department of Physics, School of Basic and Applied Sciences, RIMT University, Mandi Gobindgarh-140406, Punjab, India

³School of Physics and Materials Science, Thapar Institute of Engineering and Technology, Patiala- 147004, India

Introduction

The dynamics of nuclear reactions induced by heavy-ions lying in near barrier energy region have been a subject of great interest since decades and are specifically exploited to explore the nuclear properties for the nuclei having masses $A = 200 - 300$. In context to this, the present work aims towards carrying out the fragmentation analysis of the compound nuclei (CN) $^{219}\text{Ac}^*$ and $^{251}\text{Md}^*$ formed via ^{16}O [1] and ^{48}Ca [2] induced reactions respectively, using same target nucleus ^{203}Tl . The methodology employed here is the collective clusterization technique of Dynamical Cluster-decay Model (DCM)[3] and the analysis is carried out in terms of barrier characteristics [barrier height (V_B) and barrier position

(R_B)] and preformation probability profiles of the chosen CN.

Methodology

In DCM[3], the barrier profile is studied in terms of scattering potential which includes contribution from Coulomb potential (V_C), proximity potential (V_P) and centrifugal potential (V_ℓ), in to which the effect of deformations and temperature are duly incorporated and is given by:

$$V_R(\eta, T) = V_C(R, Z_i, \beta_{\lambda_i}, \theta_i, T) + V_P(R, A_i, \beta_{\lambda_i}, \theta_i, T) + V_\ell(R, A_i, \beta_{\lambda_i}, \theta_i, T). \quad (1)$$

The preformation probability (P_0) is obtained by solving the stationary Schrödinger equation in η , at fixed $R=R_a$:

$$\left[-\frac{\hbar^2}{2\sqrt{B_{\eta\eta}}} \frac{\partial}{\partial \eta} \frac{1}{\sqrt{B_{\eta\eta}}} \frac{\partial}{\partial \eta} + V(\eta, T) \right] \psi^\nu(\eta) = E_\eta^\nu \psi^\nu(\eta) \quad (2)$$

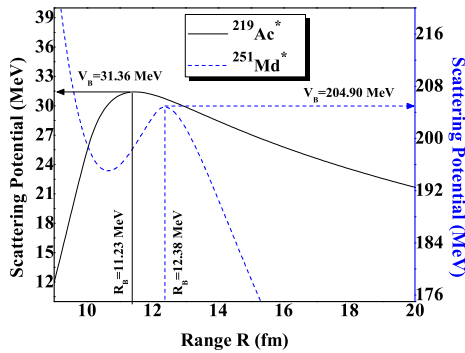


FIG. 1: Scattering potential for the $2n$ -decay channel from $^{219}\text{Ac}^*$ and $^{251}\text{Md}^*$ respectively formed via ^{16}O and ^{48}Ca induced channel.

*adeepkaur89@gmail.com

Calculations and discussions

In Fig. 1, the scattering potential for the decays $^{219}\text{Ac}^* \rightarrow ^{217}\text{Ac} + 2n$ (solid line) and $^{251}\text{Md}^* \rightarrow ^{249}\text{Md} + 2n$ (dotted line) is plotted in terms of relative separation R (fm) at respective center of mass energies $E_{c.m.} = 76.10$ MeV and $E_{c.m.} = 173.075$ MeV and best-fit values of neck-length parameter. The curve is plotted at lower values of angular momentum ($50\hbar$) because neutron evaporation is dominant at lower ℓ states only. Clearly, the barrier profiles are different for the two cases where

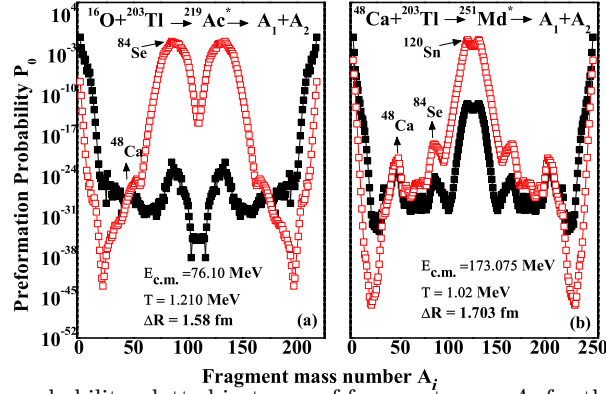


FIG. 2: Preformation probability plotted in terms of fragment mass A_i for the decay of (a) $^{219}\text{Ac}^*$ and (b) $^{251}\text{Md}^*$. The respective values of $E_{c.m.}$ and other DCM based parameters are mentioned in the figure.

the barrier height (V_B) for the lighter CN $^{219}\text{Ac}^*$ is 31.36 MeV whereas the same for heavier system is 204.90 MeV. On the other hand, the barrier position R_B is 11.23 fm and 12.38 fm, respectively, for lighter and heavier decaying CN. This difference in the barrier profile and barrier characteristics arises because of the different entrance channels- $^{16}\text{O} + ^{203}\text{Ac}$ and $^{48}\text{Ca} + ^{203}\text{Ac}$. However, notable variations might also be arising because of the difference in $E_{c.m.}$ (or T) that enters through the T-dependence of radius terms involved in defining the potential terms.

Additionally, the fragmentation behavior of the two chosen CN is compared and analyzed in terms of the preformation probability (P_0) values of all the probable exit channels from these CN in Fig. 2, where panel (a) is plotted for $^{219}\text{Ac}^*$ and (b) is plotted for $^{251}\text{Md}^*$ nucleus. The P_0 values are calculated for quadrupole deformed choice of fragments having orientations optimized for “hot” configurations and at extreme values of angular momentum ($\ell=0\hbar$ and $\ell = \ell_{max}$). The ℓ_{max} value for $^{219}\text{Ac}^*$ and $^{251}\text{Md}^*$ is $102\hbar$ and $109\hbar$ respectively. The comparative analysis of the figure indicates that for both the decaying systems, the light particle emission (LP: $A_2=1-4$) or $2n$ -emission is dominant at lower ℓ -states. Dominant maximas are arising in heavy mass region (HMF: $A_2=90\pm 10$ plus complementary region) for the $^{219}\text{Ac}^*$ while

for $^{251}\text{Md}^*$ nucleus, the peaks originate in fission region (ff: $A_2=125\pm 20$). However, the magnitude of these peaks is very less relative to that of LPs or $2n$ -emission at $\ell=0\hbar$ states and do not contribute towards decay cross-sections. As the higher ℓ -states are incorporated, structural changes are observed for both the decaying systems due to the enhancement in P_0 values of the peaks lying in HMF and ff region. The comparative analysis of the structures of $^{219}\text{Ac}^*$ and $^{251}\text{Md}^*$ systems reveals that the two systems choose different decay paths, where, $^{219}\text{Ac}^*$ undergoes asymmetric fragmentation while $^{251}\text{Md}^*$ opts for symmetric fragmentation. The origin of the asymmetric peaks in HMF region for $^{219}\text{Ac}^*$ may be attributed to the magic or near magic shell configuration for ^{84}Se and in case of $^{251}\text{Md}^*$, the symmetric fission peak may be arising due to magic shell closure at ^{120}Sn .

References

- [1] J. Gehlot et al., Phys. Rev. C **99**, 034615 (2019).
- [2] R. Biselet et al., Phys. Rev. C **99**, 024614 (2019).
- [3] R. K. Gupta, M. Bansal, Int. Rev. Phys. (I. RE. Phys.)**5**, 74, (2011); Amandeep Kaur, K. Sandhu, Gudveen Sawhney and Manoj K. Sharma, Eur. Phys. Jour. A **58:59** (2022).